THE JOURNAL OF PHYSICAL CHEMISTRY B

pubs.acs.org/JPCB Article

Linear Response Theory for Decomposition Energies of Stokes Shift in Proteins

Jirui Guo,[#] Xiaofang Wang,[#] Tanping Li,[*] and Zhiyi Wei

Cite This: *J. Phys. Chem. B* 2020, 124, 3540−3547 Read Online

ACCESS | Metrics & More | Article Recommendations

ABSTRACT: In aqueous solution, fluorescence Stokes shift experiments monitor the relaxation of the solute−solvent interactions upon photon excitation of the solute chromophore. Linear response (LR) theory expects the identical dynamics between the Stokes shift and the system's spontaneous fluctuations. Whether this identity guarantees similar dynamics between the nonequilibrated and equilibrium processes for the decomposition energy of the Stokes shift is the main focus of this study. In our previous work [Li, T. *J. Chem. Theory Comput.* **2017**, *13*, 1867−1873], Stokes shift is properly correlated with various order time-correlation functions. As a continuation, its decomposition energy from the subsystem is further represented as the full summation of all of the cross-time correlation functions between the decomposition energy and the total solute−solvent interactions. Gaussian statistics of the total solute−solvent interactions ensure the same decay rates among the odd orders not only for the time-correlation functions but also for the cross-time correlation functions, validating the LR of the Stokes shift and the decompositions, respectively. The above mechanism is verified by molecular dynamics simulations in the protein *Staphylococcus* nuclease and is robust even as the decomposed energy associated with an individual residue exhibits typical non-Gaussian properties. Further examinations reveal the consistent molecular motions for a specific residue over the nonequilibrium and equilibrium processes, which are responsible for the nonequilibrium dynamics of the associated decomposed energy. Our results show the appropriateness of LR on finer molecular scales.

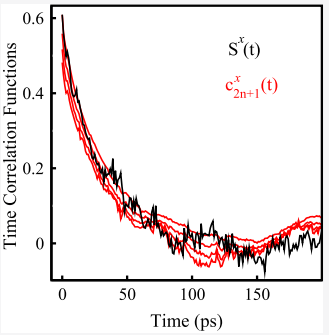

INTRODUCTION

Linear response (LR) theory has been applied extensively to study solvation dynamics in liquids.[1−9] It expects similar dynamics between the perturbed nonequilibrium process and spontaneous fluctuations of the thermally equilibrated system,[10] and forms the cornerstone to understand the intrinsic dynamics in solution. Fluorescence spectroscopic techniques investigate the response of environmental solvent molecules upon photon excitation on the solute chromophore, in which the Stokes shift monitors the relaxation of the solute−solvent interactions.[11−17] LR is applied to evaluate Stokes shift using the system's equilibrium statistics with great success,[3,18−26] even though photon excitation creates a noticeable perturbation on the system. The validities of LR are investigated extensively in the literature[8,21,22,27−35] and are believed to correlate with Gaussian statistics over the last few decades. Geissler et al. suggested that the stability of Gaussian statistics during the nonequilibrium process correlates with the efficiency of LR.[36] The studies by Thompson and co-workers recommend that the excited-state Gaussian statistics enable the LR of the Stokes shift, in which the role of higher-order time-correlation functions is stressed.[37,38] The connection between the Stokes shift and the various order time-correlation functions are further evaluated in a protein solution.[35,39,40]

Spectroscopic experiments directly monitor the relaxations of the total Stokes shift. The decomposed energies between the solute and a portion of the system are examined by theoretical investigations.[19,22,23,31,41,42] This strategy of the decompositions sheds light on the finer molecular motions of solvation dynamics, which is crucial in terms of understanding the biological functions and chemical reactions in solution. A typical example is multicomponent systems such as proteins and ionic liquids. The relaxations of the decomposed Stokes shift reveal the dynamics of hydration water and a specific residue in protein, or the dynamics of cation and anion in ionic liquid. LR for the decomposed energies probes the connection between the equilibrium fluctuations and nonequilibrium relaxations for the individual species. Yet its validity is not actively discussed as the LR of the total Stokes shift. While Gaussian statistics ensures the LR for the total solute−solvent interactions, whether it further enables LR for the decompositions? Furthermore, what is the mechanism for the LR of the decomposed Stokes shift? In the literature, the nonequilibrium dynamics of the decomposition energy are well

Received: December 12, 2019
Revised: March 25, 2020
Published: March 26, 2020

https://dx.doi.org/10.1021/acs.jpcb.9b11519
J. Phys. Chem. B 2020, 124, 3540−3547

characterized by suitably accumulating the cross-time correlation function between the decomposition and the total solute−solvent interactions over the equilibrium.[19,23,26,31,41,43] On the other hand, Schwartz and coworkers found that the underlying molecular motions are not consistent between the nonequilibrium and equilibrium processes, while the LR appears to be valid for the Stokes shift.[44] A similar phenomenon is reported that LR fails for the individual contributions from the anion and cation in ionic liquid, although efficient for the overall response of the system.[28]

In this context, we go a further step to validate the LR for the decomposed energies of the Stokes shift. In our previous investigations, the Stokes shift is explicitly evaluated as the sum of various order equilibrium time-correlation functions. LR is ensured by Gaussian statistics of the total solute−solvent interactions.[34,35,39] As a continuation of the strategy, the decomposed energies from the subsystems are properly presented as the summation of the cross-time correlation functions including higher orders, and LR is analyzed. As a first application of the formalism, molecular dynamics simulations were performed in protein *Staphylococcus* nuclease (SNase) to verify the linearity. We specifically examine the appropriateness of the LR as the energy variable associated with an individual residue exhibits typical non-Gaussian properties. Our results reveal the validity of the LR for the Stokes shift as well as its decompositions. We further verify the connection between the nonequilibrium dynamics and equilibrium properties of the system on finer molecular scales.

THEORY

Stokes Shift and Decomposition Energies. In fluorescence experiments, photon excitation produces electronic transition of a chromophore from the ground state to its excited state. The system thus undergoes nonequilibrium relaxation propagating on the excited-state surface. The Stokes shift

$$\Delta E_S(t) = \langle \delta\Delta E(t) \rangle \tag{1}$$

monitors the nonequilibrium ensemble average of the solute−solvent interactions during this process, which is defined as

$$\delta\Delta E = \beta(\Delta E - \langle \Delta E \rangle_e) \tag{2}$$

for each configuration. Here, ΔE is the energy difference between the excited and ground-state potential surface, and $\langle ... \rangle_e$ represents the excited-state equilibrium average. A scaling constant β, the Boltzmann factor, is introduced to enable $\delta\Delta E$ and the Stokes shift of the the dimensionless variables. This treatment does not hinder one to understand the inherent dynamics of the system. Solvation time-correlation is

$$S(t) = \frac{\Delta E_S(t)}{\Delta E_S(0)} \tag{3}$$

In a multicomponent system like protein solution, the Stokes shift arises from the contribution $\Delta E_S^x(t)$ of all of the subsystems by

$$\Delta E_S(t) = \sum \Delta E_S^x(t) = \sum \langle \delta\Delta E^x(t) \rangle \tag{4}$$

Here, x can be the water, protein, or a specific residue close to the chromophore. $\delta\Delta E^x$ is the contribution of the subsystem x to the total solute−solvent interactions. The normalized form of $\Delta E_S^x(t)$ is denoted in the way

$$S^x(t) = \frac{\Delta E_S^x(t)}{\Delta E_S(0)} \tag{5}$$

The solvation time-correlation function can be represented by

$$S(t) = \sum S^x(t) \tag{6}$$

Partition of the Stokes Shift and Decomposition Energy into Time-Correlation Functions and Cross-Time Correlation Functions. In the literature, the Stokes shift is equivalently evaluated by $\frac{\langle \delta\Delta E(t) e^{\delta\Delta E(0)} \rangle_e}{\langle e^{\delta\Delta E} \rangle_e}$.[2,37] In our earlier studies, $\Delta E_S(t)$ is directly correlated with various order time-correlation functions $\langle \delta\Delta E(t) \delta\Delta E(0)^n \rangle_e$ on the excited surface.[39] The latter is reformed as the relaxation of $S_n(t)$ by

$$S_n(t) = \langle \delta\Delta E(t) \delta\Delta E(0)^n \rangle_e = \int d(\delta\Delta E) \delta\Delta E(0, t) P_n(\delta\Delta E) \tag{7}$$

The above integration depicts summation over the ensemble $\delta\Delta E(0,t)$ with a certain weight, namely the weight function $P_n(\delta\Delta E)$. $\delta\Delta E(0,t)$ is interpreted as follows.[39] For a given value of $\delta\Delta E$, the related configurations are sampled over the excited-state equilibrium fluctuations. Upon evolution of the time interval t, each configuration results in a solute−solvent interaction. $\delta\Delta E(0,t)$ is referred to as the average of the above-propagated energies. The weight function is defined as

$$P_n(\delta\Delta E) = \delta\Delta E^n P_e(\delta\Delta E) \tag{8}$$

$P_e(\delta\Delta E)$ is the excited-state equilibrium distribution. As the solute−solvent interactions exhibit Gaussian statistics with $P_e(\delta\Delta E) = \frac{e^{-\delta\Delta E^2/2\sigma_e^2}}{\sqrt{2\pi\sigma_e^2}}$, the weight function can be explicitly derived as

$$P_n(\delta\Delta E) = \delta\Delta E^n \frac{e^{-\delta\Delta E^2/2\sigma_e^2}}{\sqrt{2\pi\sigma_e^2}} \tag{9}$$

Based on the above reformation, the time-correlation function can be equivalently processed by the relaxation process of $S_n(t)$, where the related dynamics are characterized by

$$c_n(t) = \frac{S_n(t)}{S_n(0)} \tag{10}$$

In the literature, the Stokes shift is revealed to arise from various order time-correlation functions.[30,37] In our previous studies, $\Delta E_S(t)$ is explicitly expressed as the summation of $S_n(t)$ with certain weights[39,40]

$$\Delta E_S(t) = \sum f_n S_n(t) = \sum f_n S_n(0) c_n(t) \tag{11}$$

The contribution of the nth order time-correlation function to the total Stokes shift is $f_n S_n(0)$. The coefficient f_n and thus the weight can be derived as follows. According to the definition in eq 7, $S_n(t)$ depicts the relaxation of $\delta\Delta E(0,t)$ with the weight function $P_n(\delta\Delta E)$. Therefore, the Stokes shift is pictured as the mixture of all of the relaxations among $S_n(t)$, in which the initial distribution $P_g(\delta\Delta E)$ of the nonequilibrium relaxation is expanded by all of the weight functions

https://dx.doi.org/10.1021/acs.jpcb.9b11519
J. Phys. Chem. B 2020, 124, 3540−3547

$$P_g(\delta\Delta E) = \sum f_n P_n(\delta\Delta E) \tag{12}$$

f_n can be derived using either the analytical or the numerical method. The solvation time-correlation function is

$$s(t) = \frac{\sum f_n S_n(0) c_n(t)}{\sum f_n S_n(0)} \tag{13}$$

The above protocol can be similarly employed on the decomposed energies. The nonequilibrium ensemble average $\langle \delta\Delta E^x(t)\rangle$ depicts the energy contribution of the subsystem x to the Stokes shift and can be evaluated by $\frac{\langle \delta\Delta E^x(t) e^{\delta\Delta E(0)}\rangle_e}{\langle e^{\delta\Delta E}\rangle_e}$.[37] The cross-time correlation $\langle \delta\Delta E^x(t)\delta\Delta E(0)^n\rangle_e$ is thus introduced by Taylor expansion. It is noted that term "cross" here refers to the time-correlation function between the decomposition $\delta\Delta E^x(t)$ and the total interaction $\delta\Delta E(0)$, which can be reformed into the relaxation of $S_n^x(t)$ by

$$\begin{aligned} S_n^x(t) &= \langle \delta\Delta E^x(t)\delta\Delta E^n\rangle_e \\ &= \int \mathrm{d}(\delta\Delta E)\, \delta\Delta E^x(0, t) P_n(\delta\Delta E) \end{aligned} \tag{14}$$

The integration illustrates the summation over the ensemble $\delta\Delta E^x(0,t)$ weighted with the initial weight function $P_n(\delta\Delta E)$. $\delta\Delta E^x(0,t)$ is the decomposition of $\delta\Delta E(0,t)$ from the subsystem x, which is the average of the propagated values of the energy quantity $\delta\Delta E^x$ (upon the time interval of t) initiated by the same $\delta\Delta E$ over the excited-state equilibrium. The following relationship naturally holds

$$S_n(t) = \sum S_n^x(t) \tag{15}$$

The normalized form, as defined in the following, obeys the certain constraint with the nth time-correlation function $c_n(t)$ by

$$\begin{aligned} c_n^x(t) &= \frac{S_n^x(t)}{S_n(0)} \\ c_n(t) &= \sum c_n^x(t) \end{aligned} \tag{16}$$

The nonequilibrium relaxation $\Delta E_S^x(t)$ is represented as the full summation over all of the cross-time correlation functions by

$$\begin{aligned} \Delta E_S^x(t) &= \sum f_n S_n^x(t) \\ &= \sum f_n S_n(0) c_n^x(t) \end{aligned} \tag{17}$$

The nth order contributes $f_n S_n(0) c_n^x(0)$ to the total energy decay $\Delta E_S^x(0)$. The decomposed solvation time-correlation function (eq 5) is thus

$$S^x(t) = \frac{\sum f_n S_n(0) c_n^x(t)}{\Delta E_S(0)} \tag{18}$$

Gaussian Statistics and Linear Response Theory. Under the circumstance of Gaussian statistics, Wick's theorem[45] enables the same decay rates among the odd order S_{2n+1} and disappearance of the even order S_{2n}, leading to the linear response theory of the Stokes shift as follows[35,39]

$$c_{2n+1}(t) = c_1(t) \tag{19}$$

$$S(t) = c_1(t) \tag{20}$$

An assumption is further made for the relaxation dynamics of S_n^x by the disappearance of S_{2n}^x for all of the even orders. The odd orders obey

$$c_{2n+1}^x(t) = c_1^x(t) \tag{21}$$

As a result, linear response theory is derived as

$$S^x(t) = c_1^x(t) \tag{22}$$

The dynamics of $\Delta E_S^x(t)$ thus depend on all of the odd orders $S_{2n+1}^x(t)$ with the identical relaxation rates. Equations 19−22 provide the key of the LR not only for the Stokes shift but also for the decomposed energies of the subsystems. The illustration of the latter has not appeared previously. It is noteworthy that the Gaussian property of $\delta\Delta E$ is desired during the above derivations, while the quantity $\delta\Delta E^x$ may not necessarily be the Gaussian random process.

We specially inspect the percentage allocation for the total energy decays, namely $\Delta E_S(0)$ and $\Delta E_S^x(0)$, in terms of the time-correlation functions and cross-time correlation functions, respectively. In eq 11, the total Stokes shift $\Delta E_S(0)$ arises from the contribution of the odd order time-correlation function by $f_{2n+1}S_{2n+1}(0)$. Similarly in eq 17, $\Delta E_S^x(0)$ arises from the contribution of the order $2n+1$ cross-time correlation function by $f_{2n+1}S_{2n+1}^x(0)$. All of the even orders contribute none as a result of Gaussian characteristics. According to eqs 19−22, the percent of the order $2n+1$ to the total energy decay obeys the following relationship

$$\frac{f_{2n+1}S_{2n+1}^x(0)}{\Delta E_S^x(0)} = \frac{f_{2n+1}S_{2n+1}(0)}{\Delta E_S(0)} \tag{23}$$

Therefore, the partitions remain the same for $\Delta E_S^x(0)$ and $\Delta E_S(0)$. The orders taking the prevailing percentages to the total Stokes shift also control the nonequilibrated dynamics of the decomposition energy. Once $S_{2n+1}(t)$ and $S_{2n+1}^x(t)$ of those orders take the same decay rates as their linear one, LR is appropriate for the Stokes shift and the decomposition energy. The percentages in eq 23 can be calculated under the circumstance of Gaussian statistics.[39] The parameter f_{2n+1} is derived based on the connection (eq 12) between the ground-state distribution $P_g(\delta\Delta E)$ and $P_n(\delta\Delta E)$; $S_{2n+1}(0)$ can be integrated by

$$S_{2n+1}(0) = \int \mathrm{d}(\delta\Delta E)\delta\Delta E^{2n+2}\frac{e^{-\delta\Delta E^2/2\sigma_e^2}}{\sqrt{2\pi\sigma_e^2}} \tag{24}$$

It is noteworthy that the percentages of some orders could be negative owing to the coefficient f_{2n+1}.

Molecular Dynamics Simulations. Tryptophan in protein is the optical probe with its indole ring as the chromophore. Molecular dynamics (MD) simulations were conducted using the GROMACS program package[46] combined with the SPC/E water model. The GROMOS96 force field[47] is applied for ground-state tryptophan. The site charges of the fluorescence state of indole were obtained by applying the ab initio partial charge density differences to the ground-state partial charges of the GROMOS96 force field.[26] The initial configuration of the protein Staphylococcus nuclease is taken from the PDB databank (1SNO). Periodic boundary conditions were implemented by using a truncated triclinic box of side length 61 Å and solvated with 4605 water molecules. The Nose−Hoover thermostat was used to maintain the system at 295 K. The initial simulations of 5 ns were

https://dx.doi.org/10.1021/acs.jpcb.9b11519
J. Phys. Chem. B 2020, 124, 3540−3547

performed to equilibrate the systems and are followed by the time length of 120 ns MD simulations on both the ground- and excited-state surfaces to probe the equilibrium statistics. Our previous investigations have found the multiple local substates originating from the energy basins on the ground-state surface.[34,35] In this context, we reveal the mechanism of LR for one of the ground-state substates, namely isomer 1, with the simulation details in accordance with refs 34 and 35.

RESULTS AND DISCUSSION

Equilibrium Distributions, Time Correlation Functions, and Cross-Time Correlation Functions. The local structure around the tryptophan W140 in protein SNase is displayed in Figure 1. This protein has been well examined by

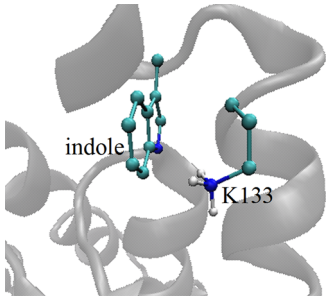

Figure 1. Local structure of protein SNase around indole W140. A positively charged K133 aligns with the indole. The spheres in color are nitrogen (blue), hydrogen (white), and carbon (cyan).

fluorescence spectroscopy[12,48] and theoretical studies.[34,35,39,48] Within 5 Å of W140, a positively charged residue K133 aligns with the nitrogen atom of the indole (Figure 1). The energy probabilities are derived based on the excited-state equilibrium simulations (Figure 2). For the total solute−solvent interaction, the distribution exhibits the Gaussian function $P_e(\delta\Delta E) = \frac{e^{-\delta\Delta E^2/2\sigma_e^2}}{\sqrt{2\pi\sigma_e^2}}$ with a variance σ_e of 3.8. For the energy

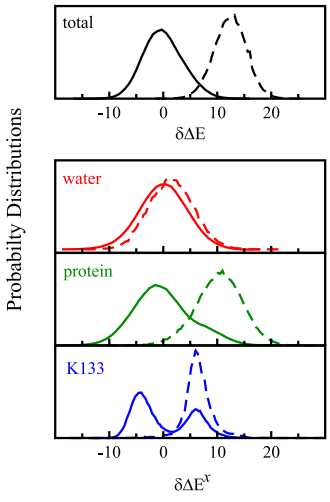

Figure 2. Probability distributions of energies on the excited state (solid lines). The total solute−solvent interactions on the top panel show the Gaussian-type profile. The decomposed contribution by protein exhibits a slight bimodal distribution, which is linked with the two clear structural alignments of the residue K133. As a comparison, the distributions over the ground-state equilibrium are also derived (dashed lines), showing a single peak for all of the energy variables.

variable $\delta\Delta E^x$ of the subsystems, the distribution profiles present diverse characteristics. The profile presents a single peak for water, and a peak at −1.2 and a slight shoulder at 4.9 for the protein, which correlate with the clear bimodal structures of the individual residue K133. As a comparison, the probabilities are also derived for $\delta\Delta E$ and $\delta\Delta E^x$ based on the ground-state (isomer 1) equilibrium fluctuation. Single peak profiles are observed for all of the energy variables, in which the distribution of the total solute−solvent interactions obeys the shifted Gaussian form $P_g(\delta\Delta E) = \frac{e^{-(\delta\Delta E-11.3)^2/2\sigma_g^2}}{\sqrt{2\pi\sigma_g^2}}$ with a σ_g of 3.0. The total energy decays of Stokes shift $\Delta E_S(0)$ and the decomposition $\Delta E_S^x(0)$ can be derived based on the ground and excited energy distributions, which is 13 for the total energy shift, 1.9 for water, 11 for the protein, and 7.7 for the residue K133.

The equilibrium dynamics of the energies are examined on the excited-state surface, which is expected to correlate with the validity of LR. For the total solute−solvent interaction $\delta\Delta E$, the time-correlation function $S_{2n+1}(t)$ is accumulated for the odd orders of 1, 3, 5, and 7 over the excited equilibrium trajectory. The statistical error makes the calculations of higher orders difficult. The normalized form $c_{2n+1}(t)$ is displayed in Figure 3. All of the curves exhibit almost identical decay rates, as characterized by an inertial drop and two exponential decays on the timescale of a few picoseconds (ps) and tens of ps. The equilibrium dynamics are also probed for the decomposed contribution $\delta\Delta E^x$ of the total solute−solvent interactions. The odd-order cross-time correlation functions of $S_{2n+1}^x(t)$ are accumulated for the water, the protein, and the residue K133. The normalized functions of $c_{2n+1}^x(t)$ are displayed in Figure 3. For all of the subsystems, the set of curves exhibit high consistency. The relaxation processes of $c_{2n+1}^x(t)$ are almost the same among the odd orders, in which the total contribution $c_{2n+1}^x(0)$ to full relaxation is 15% by water, 85% by the protein, and 59% by the residue K133. Therefore, the same decay patterns exist among the odd orders not only for the time-correlation functions but also for the cross-time correlation functions. These similarities provide straightforward evidence on Gaussian statistics and fund the linear response theory of the Stokes shift and decompositions.

LR of Stokes Shift and Decomposition Energies. By employing eq 23, we first check the energy allocations for the total Stokes shift and the decompositions with the time-correlation functions and cross-time correlation functions. Due to Gaussian statistics of $\delta\Delta E$, the percentage partition remains the same between $\Delta E_S(0)$ and $\Delta E_S^x(0)$ of the subsystem like water, the protein, and the residue K133. Figure 4 shows the percent map up to the 19th order, in which only the odd orders are present and all of the even orders contribute null. The maximum contribution arises from the 9th order with 38%. Orders 7 and 11 take 25% and 26%, respectively. These three orders take the prevailing contributions to the total energy decays by 89%. In contrast, the linear order only contributes 0.2%. Order 19 contributes 2.6%, and the contributions of higher orders are trivial. Orders 15 and 17 show slightly negative percentages, where the reasons have been illustrated in the method sessions.

Linear response theory is examined for the Stokes shift in SNase. The nonequilibrium simulations were performed by propagating 150 trajectories on the excited-state surface with the initial configurations being sampled over the ground-state

https://dx.doi.org/10.1021/acs.jpcb.9b11519
J. Phys. Chem. B 2020, 124, 3540−3547

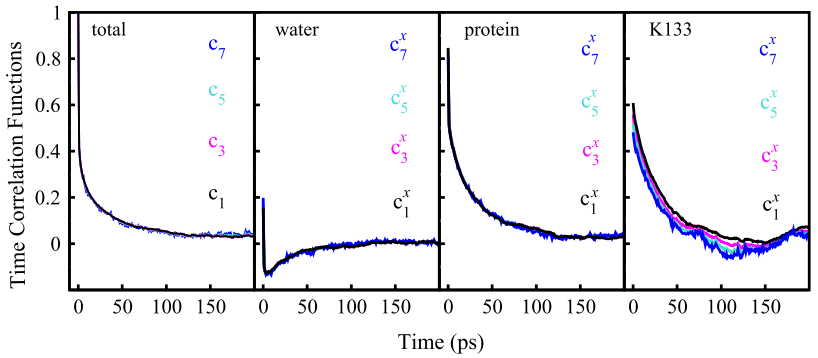

Figure 3. Normalized equilibrium time-correlation function $c_{2n+1}(t)$, labeled "total", and the cross-time correlation function $c^x_{2n+1}(t)$ for water, the protein, and the residue K133. The almost identical relaxation rates exhibit among the odd orders not only for $c_{2n+1}(t)$ but also for $c^x_{2n+1}(t)$ of all of the subsystems.

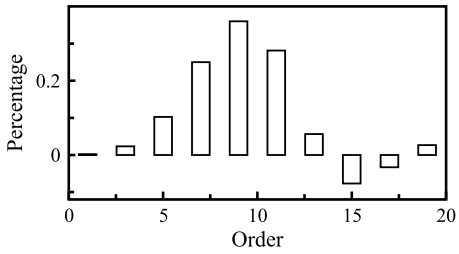

Figure 4. Percentage contributions of the odd-order time-correlation functions and cross-time correlation functions to the total decays of the Stokes shift (13) and the decomposed energy for water (1.9), protein (11) and K133 (7.7). The percentage allocations remain the same for $\Delta E_S(0)$ and $\Delta E^x_S(0)$.

equilibrium. The nonequilibrium solvation time-correlation function $S(t)$ is obtained and compared with the linear-order equilibrium time-correlation function $c_1(t)$. An excellent agreement is observed in Figure 5. LR is further examined by evaluating $S^x(t)$ for water, the protein, and the residue K133 and compared with the associated linear-order cross-time correlation function $c^x_1(t)$. For all of the subsystems, the nonequilibrium and equilibrium dynamics are in good agreement with each other. Even for the residue K133 with typical non-Gaussian properties of the bimodal energy distribution (Figure 2), the dynamics of $S^x(t)$ are still well characterized by the decay rates of $c^x_1(t)$, which undoubtedly verifies LR. The validities are mostly attributed to the equal dynamics $c_{2n+1}(t) = c_1(t)$ and $c^x_{2n+1}(t) = c^x_1(t)$ between the linear and those orders taking the prevailing percentage contributions to the total energy decays, although the dynamics of orders 9 and 11 have not been derived owing to the sampling difficulty.

We further inspect the molecular origin for the nonequilibrium relaxation of $S^x(t)$ for the residue K133. During the time interval of 200 ps upon photon excitation, the average distance between the head group of K133 and the nitrogen atom of the indole decreases from 4.5 to 3.8 Å (Figure 6A). The distance distributions during the nonequilibrium process were also obtained (Figure 6B). The profiles present a single peak at 4.5 Å at the instant of the perturbation, gradual growth of a second peak at 3.5 Å over time, and the final stabilization between the double peaks. Meanwhile, the distance fluctuations over the excited-state equilibrium are derived. Figure 6C shows that the head group of K133 hops back and forth between two states: close contact to a nitrogen atom with a distance of 3.5 Å and break up of this strong interaction. The above observations verify the coexistence of the two populations as well as their internal conversions on the excited-state surface. The structural transitions between two states occur during the nonequilibrium relaxation and account for the energy decay of $\Delta E^x_S(t)$. Correspondingly, the conversion rates correlate with the dynamics of $S^x(t)$.

CONCLUSIONS

We investigate the connection between the equilibrium and nonequilibrium solvation dynamics in optical transitions. LR is probed for both the Stokes shift and its decomposition energies. $\Delta E_S(t)$ and $\Delta E^x_S(t)$ are represented as the summation of various order time-correlation functions and cross-time

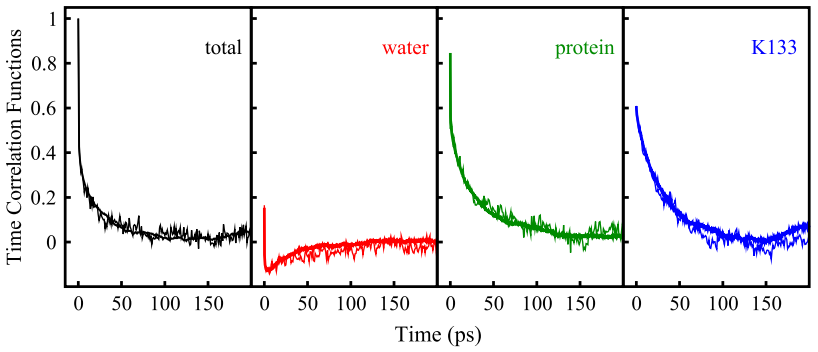

Figure 5. Comparisons between the nonequilibrium dynamics (noisy lines) of the energy decays and equilibrium time-correlation functions (smooth lines). Excellent agreements are observed between $S(t)$ and $c_1(t)$ for the total solute−solvent interactions (total), and $S^x(t)$ and $c^x_1(t)$ for water, the protein, and the residue K133, indicating the success of linear response theory.

https://dx.doi.org/10.1021/acs.jpcb.9b11519
J. Phys. Chem. B 2020, 124, 3540−3547

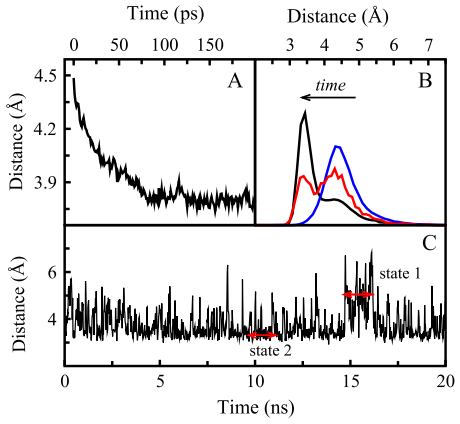

Figure 6. (A) Average distance relaxations between the head group of K133 and the nitrogen of the indole upon photon excitation; (B) time evolution of distance distribution shows a single peak at 4.5 Å on the ground-state surface (blue) and the growth of a second peak at 3.5 Å by 30 ps relaxation (red) and excited-state distribution (black); (C) equilibrium distance fluctuations extending 20 ns on the excited-state surface show the coexistence of two populations, labeled state 1 and state 2.

correlation functions, respectively. Gaussian statistics of the total solute−solvent interactions ensure the identical dynamics among the odd orders of the time-correlation functions, giving the LR of Stokes shift.[37,38] We further show the same decay rates among the odd order cross-time correlation functions under this circumstance, validating LR of the decomposition energies. Therefore, the nonequilibrium relaxations of the system upon photon excitation are correlated with its spontaneous fluctuations more than merely the Stokes shift. Our observations on the decomposition energies suggest that the dynamics on finer molecular scales are also delicately controlled by the system's equilibrium properties.

As the solute interacts with the abundant number of the surrounding solvent molecules in aqueous solution, the total solute−solvent interactions frequently exhibit Gaussian statistics, as indicated by the central limit theorem.[10,49] However, the contribution from a specific subsystem probably deviates from the Gaussian random process. This deviation does not necessarily impede the appropriateness of LR. In this study, the relaxation dynamics of the decomposition energy for an individual residue are well characterized by the equilibrium approach even with the presence of the bimodal energy distribution, which turns to be driven by the consistent molecular motions occurring over both the nonequilibrium event and the equilibrium fluctuations. On the other hand, the failure of the hidden LR theory was also reported that the underlying molecular motions responsible for the nonequilibrium relaxation differ from the ones active at equilibrium for an atomic solute in liquid tetrahydrofuran, while the LR of the Stokes shift appears to be valid.[44] This occurs because the dynamics of the nonequilibrium relaxation and the equilibrium fluctuations occur on a similar timescale and give rise to the similarity of $S(t)$ and $c_1(t)$, as revealed in a previous paper.[44] Our results are thus not in conflict with the observations in the literature.

We demonstrate a strategy to study LR for decomposition energies of the Stokes shift. The decomposed time-correlation function $c_n^x(t)$ and $S^x(t)$ can be applied to depict the equilibrium and nonequilibrium dynamics for the subsystem, which is naturally applicable for multicomponent systems as illustrated in protein. Similarly, for the ionic liquid, energy is partitioned into the contributions from the cation and the anion. LR for the individual ionic species is found valid using the fixed charge molecules[31] and not accurate in polarizable molecule simulations.[28] The underlying mechanism can be probed using the theory in this context. Beyond the above multicomponent systems, the method is expected to have a more general application on solvation dynamics, once the appropriate decompositions of energies are performed. For example, Schwartz et al. introduced a protocol to project the total interaction $\delta\Delta E$ into the contribution from a molecule's translation and rotation (including cross-terms) for the atomic solute in liquid tetrahydrofuran.[44] The decomposition enables the deriving of the associated $c_n^x(t)$ and $S^x(t)$ and thus evaluating the dynamics for the explicit molecular motions over the equilibrium fluctuations and nonequilibrium relaxations. Further efforts are desired to apply LR of the decomposition energies in understanding solvation dynamics.

AUTHOR INFORMATION

Corresponding Author

Tanping Li − *School of Physics and Optoelectronic Engineering, Xidian University, Xi'an 710071, People's Republic of China;* orcid.org/0000-0002-2164-2673; Email: tpli@xidian.edu.cn

Authors

Jirui Guo − *School of Physics and Optoelectronic Engineering, Xidian University, Xi'an 710071, People's Republic of China*

Xiaofang Wang − *School of Physics and Optoelectronic Engineering, Xidian University, Xi'an 710071, People's Republic of China*

Zhiyi Wei − *Beijing National Laboratory for Condensed Matter Physics, Institute of Physics, Chinese Academy of Sciences, Beijing 100190, China;* orcid.org/0000-0001-9052-6732

Complete contact information is available at: https://pubs.acs.org/10.1021/acs.jpcb.9b11519

Author Contributions

#Equal contribution (J.G. and X.W.).

Notes

The authors declare no competing financial interest.

ACKNOWLEDGMENTS

This work was supported by the National Natural Science Foundation of China (Grant No. 11974267), the Natural Science Foundation of Shaanxi Provincial Department of Education (Grant No. 2019JM-556), and the 111 Project under Grant No. B17035.

REFERENCES

(1) Maroncelli, M.; Fleming, G. R. Computer-Simulation of the Dynamics of Aqueous Solvation. *J. Chem. Phys.* **1988**, *89*, 5044−5069.

(2) Carter, E. A.; Hynes, J. T. Solvation Dynamics for an Ion-Pair in a Polar-Solvent - Time-Dependent Fluorescence and Photochemical Charge-Transfer. *J. Chem. Phys.* **1991**, *94*, 5961−5979.

(3) Fonseca, T.; Ladanyi, B. M. Breakdown of Linear Response for Solvation Dynamics in Methanol. *J. Phys. Chem. A* **1991**, *95*, 2116−2119.

(4) Schwartz, B. J.; Rossky, P. J. Aqueous Solvation Dynamics with a Quantum-Mechanical Solute - Computer-Simulation Studies of the Photoexcited Hydrated Electron. *J. Chem. Phys.* **1994**, *101*, 6902−6916.

(5) Stratt, R. M.; Maroncelli, M. Nonreactive Dynamics in Solution: The Emerging Molecular View of Solvation Dynamics and Vibrational Relaxation. *J. Phys. Chem. B* **1996**, *100*, 12981−12996.
(6) Skaf, M. S.; Ladanyi, B. M. Molecular Dynamics Simulation of Solvation Dynamics in Methanol-Water Mixtures. *J. Phys. Chem. C* **1996**, *100*, 18258−18268.
(7) Turi, L.; Minary, P.; Rossky, P. J. Non-linear Response and Hydrogen Bond Dynamics for Electron Solvation in Methanol. *Chem. Phys. Lett.* **2000**, *316*, 465−470.
(8) Moskun, A. C.; Jailaubekov, A. E.; Bradforth, S. E.; Tao, G. H.; Stratt, R. M. Rotational Coherence and a Sudden Breakdown in Linear Response Seen in Room-Temperature Liquids. *Science* **2006**, *311*, 1907−1911.
(9) Floisand, D. J.; Corcelli, S. A. Computational Study of Phosphate Vibrations as Reporters of DNA Hydration. *J. Phys. Chem. Lett.* **2015**, *6*, 4012−4017.
(10) Chandler, D. *Introduction to Modern Statistical Mechanics*; Oxford University Press, 1987; pp 114−118.
(11) Pal, S. K.; Zewail, A. H. Dynamics of Water in Biological Recognition. *Chem. Rev.* **2004**, *104*, 2099−2123.
(12) Qiu, W.; Kao, Y. T.; Zhang, L.; Yang, Y.; Wang, L.; Stites, W. E.; Zhong, D.; Zewail, A. H. Protein Surface Hydration Mapped by Site-Specific Mutations. *Proc. Natl. Acad. Sci. U.S.A.* **2006**, *103*, 13979−13984.
(13) Zhang, L.; Wang, L.; Kao, Y. T.; Qiu, W.; Yang, Y.; Okobiah, O.; Zhong, D. Mapping Hydration Dynamics around a Protein Surface. *Proc. Natl. Acad. Sci. U.S.A.* **2007**, *104*, 18461−18466.
(14) Waegele, M. M.; Culik, R. M.; Feng, G. Site-Specific Spectroscopic Reporters of the Local Electric Field, Hydration, Structure, and Dynamics of Biomolecules. *J. Phys. Chem. Lett.* **2011**, *2*, 2598−2609.
(15) Nibali, V. C.; Havenith, M. New Insights into the Role of Water in Biological Function: Studying Solvated Biomolecules Using Terahertz Absorption Spectroscopy in Conjunction with Molecular Dynamics Simulations. *J. Am. Chem. Soc.* **2014**, *136*, 12800−12807.
(16) Qin, Y.; Jia, M.; Jin, Y.; Wang, D.; Wang, L.; Xu, J.; Zhong, D. Molecular Origin of Ultrafast Water−Protein Coupled Interactions. *J. Phys. Chem. Lett.* **2016**, 4171−4177.
(17) Qin, Y.; Wang, L.; Zhong, D. Dynamics and Mechanism of Ultrafast Water-Protein Interactions. *Proc. Natl. Acad. Sci. U.S.A.* **2016**, *113*, 8424−8429.
(18) Aherne, D.; Vu Tran, A.; Schwartz, B. J. Nonlinear, Nonpolar Solvation Dynamics in Water: The Roles of Electrostriction and Solvent Translation in the Breakdown of Linear Response. *J. Phys. Chem. B* **2000**, *104*, 5382−5394.
(19) Nilsson, L.; Halle, B. Molecular Origin of Time-Dependent Fluorescence Shifts in Proteins. *Proc. Natl. Acad. Sci. U.S.A.* **2005**, *102*, 13867−13872.
(20) Shim, Y.; Choi, M. Y.; Kim, H. J. A Molecular Dynamics Computer Simulation Study of Room-Temperature Ionic Liquids. II. Equilibrium and Nonequilibrium Solvation Dynamics. *J. Chem. Phys.* **2005**, *122*, No. 044511.
(21) Tao, G. H.; Stratt, R. M. The Molecular Origins of Nonlinear Response in Solute Energy Relaxation: The Example of High-Energy Rotational Relaxation. *J. Chem. Phys.* **2006**, *125*, No. 114501.
(22) Golosov, A. A.; Karplus, M. Probing Polar Solvation Dynamics in Proteins: A Molecular Dynamics Simulation Analysis. *J. Phys. Chem. B* **2007**, *111*, 1482−1490.
(23) Furse, K. E.; Lindquist, B. A.; Corcelli, S. A. Solvation Dynamics of Hoechst 33258 in Water: An Equilibrium and Nonequilibrium Molecular Dynamics Study. *J. Phys. Chem. B* **2008**, *112*, 3231−3239.
(24) Furse, K. E.; Corcelli, S. A. Dynamical Signature of Abasic Damage in DNA. *J. Am. Chem. Soc.* **2011**, *133*, 720−723.
(25) Kim, D.; Park, S. W.; Shim, Y.; Kim, H. J.; Jung, Y. J. Excitation-Energy Dependence of Solvation Dynamics in Room-Temperature Ionic Liquids. *J. Chem. Phys.* **2016**, *145*, No. 044502.
(26) Li, T.; Hassanali, A. A.; Singer, S. J. Origin of Slow Relaxation Following Photoexcitation of W7 in Myoglobin and the Dynamics of Its Hydration Layer. *J. Phys. Chem. B* **2008**, *112*, 16121−16134.
(27) Heid, E.; Schröder, C. Solvation Dynamics in Polar Solvents and Imidazolium Ionic Liquids: Failure of Linear Response Approximations. *Phys. Chem. Chem. Phys.* **2018**, *20*, 5246−5255.
(28) Heid, E.; Schröder, C. Polarizability in Ionic Liquid Simulations Causes Hidden Breakdown of Linear Response Theory. *Phys. Chem. Chem. Phys.* **2019**, *21*, 1023−1028.
(29) Heid, E.; Moser, W.; Schröder, C. On the Validity of Linear Response Approximations Regarding the Solvation Dynamics of Polyatomic Solutes. *Phys. Chem. Chem. Phys.* **2017**, *19*, 10940−10950.
(30) Schile, A. J.; Thompson, W. H. Tests for, Origins of, and Corrections to Non-Gaussian Statistics. The Dipole-Flip Model. *J. Chem. Phys.* **2017**, *146*, No. 154109.
(31) Terranova, Z. L.; Corcelli, S. A. Decompositions of Solvent Response Functions in Ionic Liquids: A Direct Comparison of Equilibrium and Nonequilibrium Methodologies. *J. Phys. Chem. B* **2018**, *122*, 6823−6828.
(32) Bragg, A. E.; Cavanagh, M. C.; Schwartz, B. J. Linear Response Breakdown in Solvation Dynamics Induced by Atomic Electron-Transfer Reactions. *Science* **2008**, *321*, 1817−1822.
(33) Bedard-Hearn, M. J.; Larsen, R. E.; Schwartz, B. J. Projections of Quantum Observables onto Classical Degrees of Freedom in Mixed Quantum-Classical Simulations: Understanding Linear Response Failure for the Photoexcited Hydrated Electrony. *Phys. Rev. Lett.* **2006**, *97*, No. 130403.
(34) Li, T. Validity of Linear Response Theory for Time-Dependent Fluorescence in Staphylococcus Nuclease. *J. Phys. Chem. B* **2014**, *118*, 12952−12959.
(35) Li, T.; Kumar, R. Role of Excited State Solvent Fluctuations on Time-Dependent Fluorescence Stokes Shift. *J. Chem. Phys.* **2015**, *143*, No. 174501.
(36) Geissler, P. L.; Chandler, D. Importance Sampling and Theory of Nonequilibrium Solvation Dynamics in Water. *J. Chem. Phys.* **2000**, *113*, 9759−9765.
(37) Laird, B. B.; Thompson, W. H. On the Connection between Gaussian Statistics and Excited-State Linear Response for Time-Dependent Fluorescence. *J. Chem. Phys.* **2007**, *126*, No. 211104.
(38) Laird, B. B.; Thompson, W. H. Time-Dependent Fluorescence in Nanoconfined Solvents: Linear-Response Approximations and Gaussian Statistics. *J. Chem. Phys.* **2011**, *135*, No. 084511.
(39) Li, T. Efficient Criterion To Evaluate Linear Response Theory in Optical Transitions. *J. Chem. Theory Comput.* **2017**, *13*, 1867−1873.
(40) Li, T.; Wang, X. Theoretical Insights on Nonlinear Response Theory of Fluorescence Spectroscopy in Liquids. *J. Chem. Theory Comput.* **2019**, *15*, 471−476.
(41) Li, T.; Hassanali, A. A.; kao, Y. T.; Zhong, D.; Singer, S. J. Hydration Dynamics and Time Scales of Coupled Water-Protein Fluctuations. *J. Am. Chem. Soc.* **2007**, *129*, 3376−3382.
(42) Furse, K. E.; Corcelli, S. A. Molecular Dynamics Simulations of DNA Solvation Dynamics. *J. Phys. Chem. Lett* **2010**, *1*, 1813−1820.
(43) Furse, K. E.; Corcelli, S. A. Effects of Long-Range Electrostatics on Time-Dependent Stokes Shift Calculations. *J. Chem. Theory Comput.* **2009**, *5*, 1959−1967.
(44) Bedard-Hearn, M. J.; Larsen, R. E.; Schwartz, B. J. Hidden Breakdown of Linear Response: Projections of Molecular Motions in Nonequilibrium Simulations of Solvation Dynamics. *J. Phys. Chem. A* **2003**, *107*, 4773−4777.
(45) Wick, G. C. The Evaluation of the Collision Matrix. *Phys. Rev.* **1950**, *80*, 268−272.
(46) Lindahl, E.; Hess, B.; Van Der Spoel, D. GROMACS 3.0: A Package for Molecular Simulation and Trajectory Analysis. *Mol. Model. Annu.* **2001**, *7*, 306−317.
(47) Scott, W. R. P.; Hünenberger, P. H.; Tironi, I. G.; Mark, A. E.; Billeter, S. R.; Fennen, J.; Torda, A. E.; Huber, T.; Peter Krüger, A.; Gunsteren, W. F. V. The GROMOS Biomolecular Simulation Program Package. *J. Phys. Chem. A* **1999**, *103*, 3596−3607.

https://dx.doi.org/10.1021/acs.jpcb.9b11519
J. Phys. Chem. B 2020, 124, 3540−3547

(48) Scott, J. N.; Callis, P. R. Insensitivity of Tryptophan Fluorescence to Local Charge Mutations. *J. Phys. Chem. B* **2013**, *117*, 9598−9605.
(49) Khinchin, A. I. *Mathematical Foundations of Statistical Mechanics*; Dover Publications: New York, 1949.

https://dx.doi.org/10.1021/acs.jpcb.9b11519
J. Phys. Chem. B 2020, 124, 3540−3547